

# Robust Adaptive Control of Permanent Magnetic Suspension System Using Variable Flux Path Control Method

Feng SUN\*, Pengpeng XIA\*, Xingwei SUN\*, He LU\*, Koichi OKA\*\*

\*School of Mechanical Engineering, Shenyang University of Technology, Shenyang, China,

E-mail: [sunfeng@sut.edu.cn](mailto:sunfeng@sut.edu.cn)

\*\*Intelligent Mechanical Systems Engineering, Kochi University of Technology, Kochi, Japan,

## Abstract

In order to reduce the power consumption of magnetic suspension system, a magnetic suspension system using variable flux path control method was put forward. And, to stabilize the system, the robust control model is established and status feedback  $\gamma$  suboptimal  $H_\infty$  robust controller is designed by  $H_\infty$  robust control method basing the LMI. Suspension characteristics were analyzed using numerical simulation and experiment, in which the simulation was based on the Matlab/simulink and the experiment was based on the single degree freedom magnetic suspension system. The results show that the suspension system can realize the saving energy suspension, respond displacement input signal. Besides, for the system has a nonlinear characteristic, a static feedback robust controller cannot guarantee the system stability, when the air gap was changed so much. And in order to solve this problem, the adaptive control idea was applied into the system, a robust adaptive control method is proposed. And the robust adaptive control was applied into the suspension system. The simulation and experiment results proved that the controller can obtain a large controllable air gap in a stable suspension state.

**Keywords:** Magnetic suspension, Variable flux path control, Robust control, Adaptive control, Linear Matrix Inequality

## 1. Introduction

Until now, many magnetic suspension systems have been proposed<sup>[1]-[3]</sup>. They can mainly be divided into the following categories: electromagnetic suspension system<sup>[4]</sup>, permanent magnet suspension system<sup>[5]</sup>, hybrid suspension of electromagnets and others.

For the magnetic suspension technique has the characteristics of non-contacting, non-friction and high precision, it was widely applied to many industrial applications. Such as maglev train, magnetic bearing, maglev linear motor and so on. And since the traditional electromagnetic suspension technology with the shortage of high energy consumption, to satisfy the requirements of low-power consumption and energy conservation, more and more permanent magnetic suspension technology were applied to practice gradually. Such as permanent-magnet bias radial magnetic bearing, hybrid-levitation system with permanent magnets and electro-magnets .....

According to the nonlinear and strong coupling characteristics of the magnetic suspension system<sup>[7]-[8]</sup>, many kinds of control methods were used in the controller design and have achieved good results. Such as  $H_\infty$  robust control method, self-adaption control method<sup>[9]</sup>, fuzzy control method<sup>[10]</sup>.....

The author has proposed a permanent magnetic suspension system using variable flux path control method<sup>[11]</sup>. Since the suspension system has the nonlinear characteristic, a static controller cannot obtain a large controllable air gap in a stable suspension state.

A robust control model is established and status feedback  $\gamma$  suboptimal  $H_\infty$  robust controller is designed by  $H_\infty$  robust control method basing the LMI. Then, according to the design idea of robust control and adaptive control, a robust adaptive control method is proposed to solve the problem in this paper.

## 2. Principle of variable flux path control mechanism

The permanent magnetic suspension system is mainly composed of a disk permanent magnet, a rotary actuator (servo motor), two opposite F-type iron cores and a suspended object. The principle of the system can be explained by

figure1. No magnet flux passing through the suspension object, then there would be no attractive force between iron cores and suspended object when the rotation angle of the disk magnet is zero. Once the rotation angle is changed (Driven by the motor), the magnetic flux can pass through the suspended object and the attractive force is generated.

When the attractive force is equal to the gravity of the suspended object, the suspended object would be suspended. At this time, the rotary actuator would adjust the angel of permanent magnet to offset the small disturbance around the equilibrium position and keep the balance of suspended object.

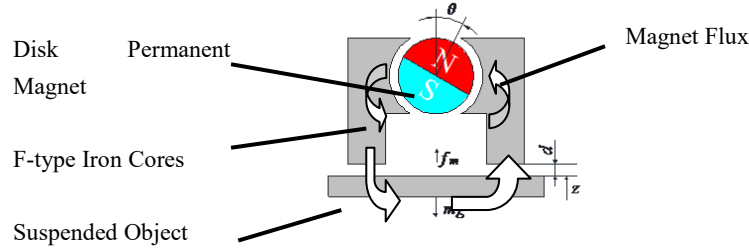


Figure1 Principle of the system

### 3. Mathematical model

According to the Figure 1, the mathematical model are referred as follows,

$$f_m = k_m \frac{\sin^2 \theta}{(d + \Delta d_f)^2} \quad (1)$$

$$T_L = k_\tau \frac{\sin 2\theta}{d + \Delta d_\tau} \quad (2)$$

Where  $f_m$  is the attractive force,  $T_L$  is the rotation torque of disk magnet,  $k_m$  is the coefficient of attractive force and the  $\Delta d_f$  is the compensation coefficient of air gap length of attractive force,  $k_\tau$  is the proportion coefficient of rotation torque and the  $\Delta d_\tau$  is the compensation coefficient of air gap length of rotation torque,  $d$  is the air gap length,  $\theta$  is the rotation angel of magnet.

According to equation (1) and (2), the system dynamical equations are referred as follows,

$$m\ddot{z} = \frac{2k_m (\sin \theta_0)^2}{(d_0 + \Delta d_f)^3} z + \frac{k_m \sin 2\theta_0}{(d_0 + \Delta d_f)^2} \Delta\theta + c_1 \dot{z} + f_d \quad (3)$$

$$J\Delta\ddot{\theta} = c_2 \Delta\dot{\theta} + \frac{k_\tau \sin 2\theta_0}{(d_0 + \Delta d_\tau)^2} z + \frac{2k_\tau \cos 2\theta_0}{d_0 + \Delta d_\tau} \Delta\theta + k_i \Delta i \quad (4)$$

Where  $z$  is the small displacement around the equilibrium position( $d_0$ ), and  $d = d_0 - z$ ,  $c_1$  is the damping coefficient in vertical motive direction,  $f_d$  is the disturbing force,  $c_2$  is the damping coefficient of servo motor,  $k_i$  is the torque coefficient of servo motor,  $J$  is the rotational inertia,  $i$  is the input current of serve motor.

The mainly parameters of the suspension system are shown in table 1. And all the simulations and experiments were based on these parameters.

Tab. 1 The parameters of suspension system

Parameter	Value
The mass of suspended object $m$ /(kg)	0.262
The compensation coefficient of air gap length of rotation torque $\Delta d_\tau$ /(mm)	14

The compensation coefficient of air gap length of attractive force $\Delta d_f$ (mm)	1.6
The damping coefficient in vertical motive direction $c_1$ (N/(m/s))	0.5
The damping coefficient of servo motor $c_2$ (N/(m/s))	100
The rotational inertia $J$ (kg·m <sup>2</sup> )	$6.37 \times 10^{-4}$
The torque coefficient of servo motor $k_t$ (Nm/A)	0.69
The coefficient of attractive force $k_m$ (Nm <sup>2</sup> )	$2.45 \times 10^{-4}$
The proportion coefficient of rotation torque $k_\tau$ (Nm <sup>2</sup> )	$-8.726 \times 10^{-3}$

#### 4. Design of $H_\infty$ robust controller

Through linearizing the dynamical equations around the equilibrium position, the extended state space equation is represented.

$$\begin{cases} \dot{x} = Ax + B_2 w + B_1 \Delta i \\ z_1 = C_1 x + D_{11} w + D_{12} \Delta i \\ y = C_2 x \end{cases} \quad (5)$$

$$x = (z \quad \dot{z} \quad \Delta \theta \quad \Delta \dot{\theta})^T$$

Where,  $z_1$  is the output evaluation signal,  $C_1$ 、 $D_{11}$  and  $D_{12}$  are the state weighting matrixes,  $C_2$  is the output matrix. And assuming that  $D_{11}$  is the zero matrix in the state space equation.

In order to obtain the static state feedback robust controller of this system, a linear matrix inequality (LMI) for this system was introduced i.e.,

$$\begin{cases} \min \gamma \\ \begin{bmatrix} AX + B_2 W + (AX + B_2 W)^T & B_1 & (C_1 X + D_{12} W)^T \\ B_1^T & -I & D_{11} \\ C_1 X + D_{12} W & D_{11} & -\gamma^2 I \end{bmatrix} < 0 \\ X > 0 \end{cases} \quad (6)$$

Only the feasible solution of  $X^*$  and  $W^*$  were existed, can we gain the controller  $K=W^*(X^*)^{-1}$ . It is a state feedback  $\gamma$  suboptimal  $H_\infty$  controller.

An M-function was established to solve the inequality (6) based on Matlab. Thus, the state feedback controller  $K=[K1 \ K2 \ K3 \ K4]$  was calculated through  $H_\infty$  robust control strategy which is based on LMI (Linear Matrix Inequation). And the system can satisfy the control performance requirement around the equilibrium position with this controller.

#### 5. Design of adaptive robust controller

The relationship between attractive force  $f_m$ 、air gap length  $d$  and input current  $i$  is obtained, from Eq.(1) and (2).

$$i = \frac{2k_\tau(d + d_f)}{k_t(d + d_\tau)} \sqrt{\frac{f_m}{k_m} - \frac{f_m^2}{k_m^2}} (d + d_f)^2 \quad (7)$$

Then, the relationship between rotation angel and input current in different attractive force was obtained and shown in Figure 2.

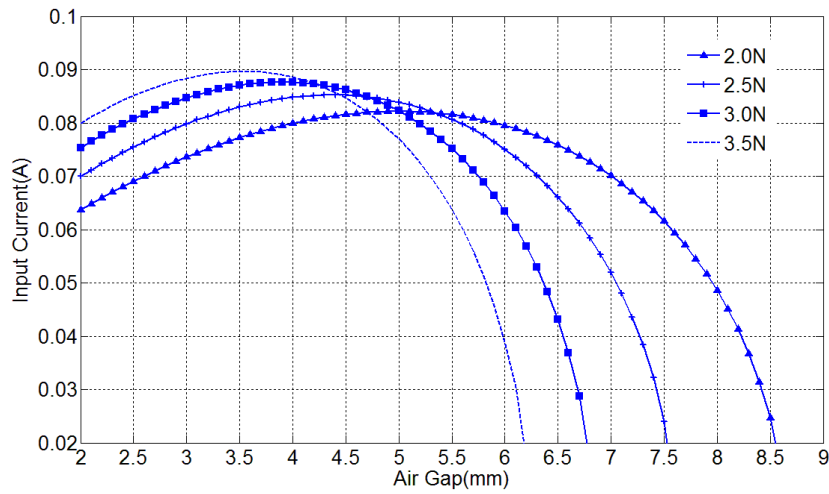


Figure 2 The relationship between air gap and input current in different attractive force

The results indicate that the relationship between Air gap and input current is nonlinear in general. However, it is almost linear in some certain areas. In order to make the suspended object suspended and moved in a stable state in larger goal workspace, the variation displacement feedback coefficient is indispensability.

Table 2 shows the parameters of the above robust controller in different air gap position, which have been proved by experiment.  $K_1$ ,  $K_2$ ,  $K_3$ ,  $K_4$  are the feedback coefficients of displacement, velocity, angel, angular velocity respectively. The results shown in table 2 suggest that the variation of air gap has great relationship with  $K_1$  and has little relationship with other feedback coefficients.

Tab. 2 The parameters of robust controller in different air gap positions

Air Gap(mm)	$K_1$	$K_2$	$K_3$	$K_4$
3	200000	700	400	2.5
4	225000	700	400	2.5
5	240000	660	400	2.5
6	266000	660	400	2.5
7	280000	670	400	2.5

Then the adaptive robust controller was obtained, with adjusting  $K_1$  by air gap. And the position in 5mm air gap was regarded as the middle position. The gains of adaptive controller was  $K=[280000-(0.007-d)*20000,660,400,2.5]$ . The air gap varied from 3.5mm to 7.5mm.

## 6. Simulation

### 6.1 Step displacement signal tracking

In order to study the  $H_\infty$  robust controller's feasibility, a simulation of step signal tracking was carried out. And the displacement  $z$ , rotation angel  $\theta$  and input current  $i$  were tracked and shown in Figure 4.

In the figure, we can conclude that the system suspended object can track the step signal and the controller can guarantee the system with a stable operation. At first, the suspend object was in the equilibrium position with the air gap 5mm, displacement  $z$  0mm, rotation angel of permanent magnet  $52^\circ$  and input current 0.06 A. Then a 0.07mm reference step displacement signal of suspended object was applied to the system. After this, the displacement of suspended object, the rotation angel of permanent magnet and the input current of servo motor were changed and then reached to stable values. The final value of displacement was bigger than the initial value. The rotation angel of permanent magnet was smaller than the initial value. The final value of input current of servo motor was almost same as the initial value.

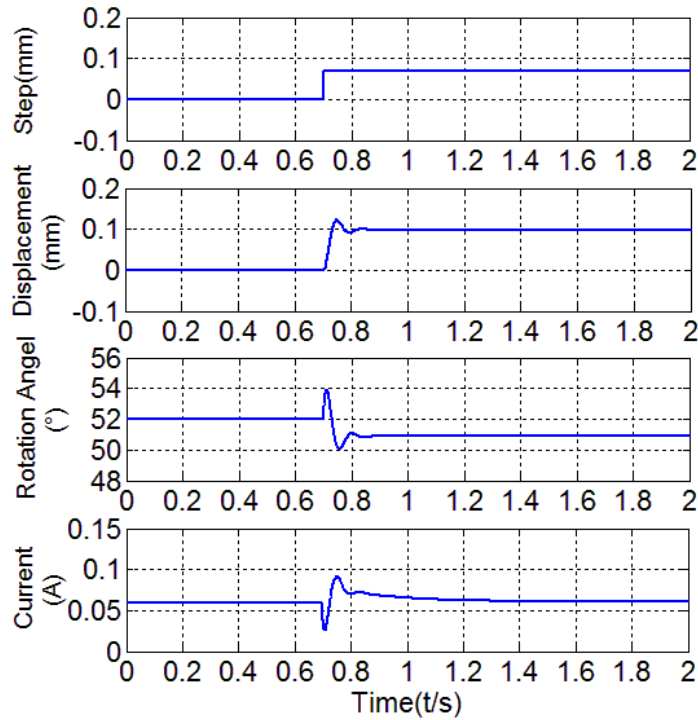


Figure 4 Simulation of step displacement signal tracking

### 6.2 Slope displacement signal tracking

In order to study the controller's feasibility, a simulation was carried out to realize the process of moving the suspended object back and forth in an air gap from 3.5mm to 7.5 mm. And the value of Gain(K1), Air Gap, Rotation Angel and Input current  $i$  were tracked.

Figure 5 shows the simulation results. At first, the reference value of air gap was remained unchanged, and then it was decreased, after this, it was reached to a minimum value. At last, it was increased and return to initial value. The gain (K1), rotation angel of permanent magnet and air gap had the same variation tendency with the reference value of air gap. While the input current of servo had the completely opposite variation tendency with the reference value of air gap.

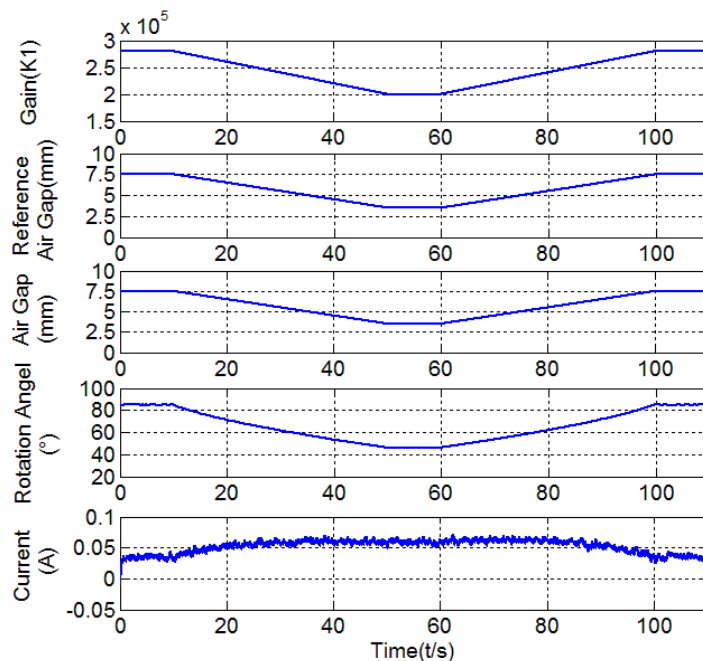


Figure5 Simulation of slop displacement signal tracking

## 7. Experiment

### 7.1 Experimental platform

Figure 6 shows the single degree freedom magnetic suspension platform with variable flux path control. In the picture, the suspended object was in the suspended state with an air gap of about 5mm.

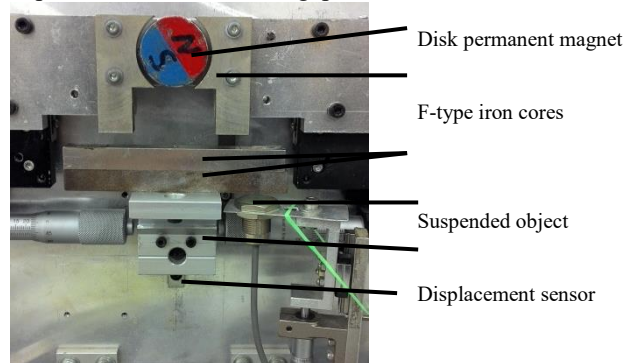


Figure 6 Experimental platform

Where, the two opposite F-type iron cores were located on either side of the radial magnetic disk permanent magnet; the disk permanent magnet was connected with the DC servo motor with a coupling; the DC servo motor was behind the disk permanent magnet; in order to adjust the weight of suspended object, the suspended object was composed of several magnetizer, and was connected with a slide; the linear guide pair was to balance the torque which was produced by the two opposite F-type iron cores; the eddy current displacement was under the suspended object to measure displacement; the dSPACE was regard as the core control hardware.

### 7.2 Step displacement signal tracking

In order to study the  $H_\infty$  robust controller's feasibility, a experiment of step signal tracking was carried out. And the displacement sensor value, rotation angel  $\theta$  and input current  $i$  were tracked and shown in Figure 7.

The experiment results were almost agreed with the simulations results. However, for the performance of experimental equipment was not that good and the simplified modeling, the system response curves were not smooth, all the parameters were vibrated around the equilibrium position when the system was in equilibrium state.

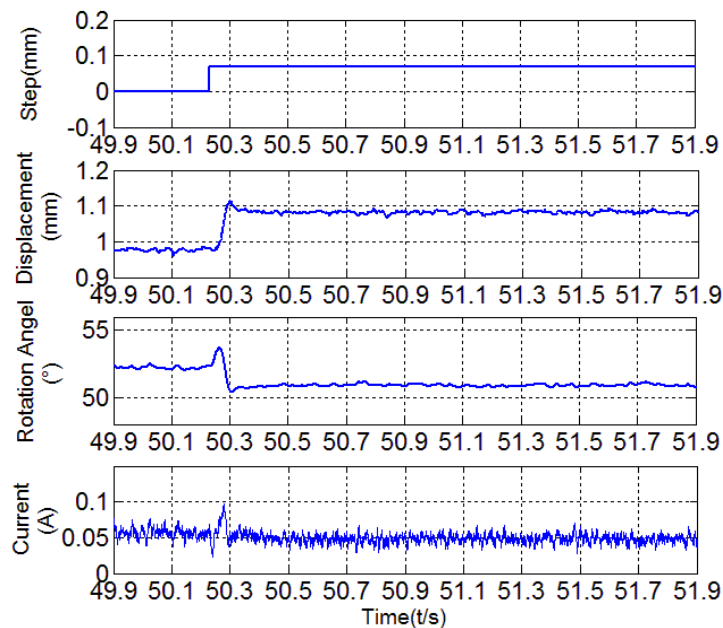


Figure 7 Experiment of step displacement signal tracking

### 7.3 Slop displacement signal tracking

Figure 8 shows the experiment results of slop displacement signal tracking.

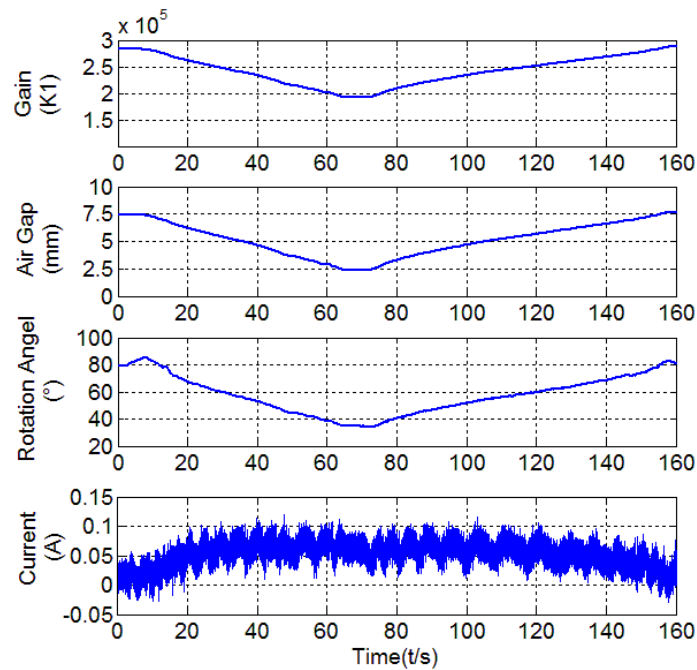


Figure 8 Experiment of slop displacement signal tracking

The moving process was almost agreed with the simulation results. However, the ramp reference input was entered manually. The slope of reference displacement curve could not be guaranteed. Then other slope of parameters could not be guaranteed at the same time. The respond curves became much unsmooth.

According to the simulation and experiment, the robust adaptive controller was proved to be useful in this system.

## 8. Conclusion

In the paper, to stabilize the system, the robust control model is established and status feedback  $\gamma$  suboptimal  $H_\infty$  robust controller is designed by  $H_\infty$  robust control method basing the LMI. Then, according to the design idea of robust control method and adaptive control method, a robust adaptive controller for a permanent magnetic suspension system was proposed. The simulation and experiment results proved that the robust adaptive controller can obtain a large controllable air gap in a stable suspension state.

## 9. References

- [1] M. Morishita, et al., A new Maglev system for magnetically levitated carrier system, IEEE Transaction Vehicular Technology, Vol. 38, No. 4(1989), pp. 230-236.
- [2] Post R F and Ryutor D D, The inductrack: a simpler approach to magnetic levitation, IEEE Transaction on Applied Superconductivity, Vol. 10, No. 1(2000), pp. 901-904.
- [3] T. Ueno and T. Higuchi, Zero-Power Magnetic Levitation Using Composite of Magnetostrictive Piezoelectric Material, Transactions on Magnetics, Vol. 437, No. 8(2007), pp. 3477-3482.
- [4] Lan Yipeng, et al., Robust Control of Direct Magnetic Suspension Permanent Magnet Linear Motor, Transactions of China Electro-technical Society, Vol. 26, No. 5(2011), pp. 132-137.
- [5] Oka K, Noncontact Manipulation with Permanent Magnet Motion Control, Proceeding of the 4th International Symposium on Linear Drivers for Industry Applications, CDROM: 259~262.
- [6] Chen Huixing, et al., Research on Levitation Stiffness of Hybrid Suspension System, Proceedings of the CSEE, (2008), pp.148-152.
- [7] Queizroz deM and Dawson D, Nonlinear Control of Active Magnetic Bearings: A Backstepping Approach, IEEE Transactions on Control Systems Technology, Vol. 4, No. 5(1996), pp. 545-552.
- [8] Charara A, et al., Nonlinear Control of a Magnet Levitation System without Premagnetization, IEEE Transactions on Control Systems, Vol. 4, No. 5(1996), pp. 513-523.

- [9] Li Yungang, et al., Research on Adaptive Control Method of Hybrid Maglev System, Electric Drive for Locomotives, No. 2(2007), pp. 33-35.
- [10] Qu Pingping and Wei Shaoyi, Fuzzy Controller Design for Magnetic Floating Systems, Control Engineering of China, No. 13(2006), pp. 78-80.
- [11] Sun Feng and Oka Koichi, Development of Noncontact Suspension Mechanism Using Flux Path Control Disk Magnet Rotation, Transactions of the Japan Society of Mechanical Engineers, Vol. 76, No. 771(2010), pp. 2916-2922.